Human Mig Chemokine: Biochemical and Functional Characterization

By Fang Liao,* Ronald L. Rabin,* John R. Yannelli,‡
Leonidas G. Koniaris,§ Padmavathy Vanguri,§ and Joshua M. Farber*

*From the *Laboratory of Clinical Investigation, National Institute of Allergy and Infectious Diseases and the ‡Surgery Branch, National Cancer Institute, National Institutes of Health, Bethesda, Maryland 20892; and the §Johns Hopkins University School of Medicine, Baltimore, Maryland 21205*

Summary

Mig is a chemokine of the CXC subfamily that was discovered by differential screening of a cDNA library prepared from lymphokine-activated macrophages. The *mig* gene is inducible in macrophages and in other cells in response to interferon (IFN)-γ. We have transfected Chinese hamster ovary (CHO) cells with cDNA encoding human Mig and we have derived CHO cell lines from which we have purified recombinant human Mig (rHuMig). rHuMig induced the transient elevation of $[Ca^{2+}]_i$ in human tumor-infiltrating T lymphocytes (TIL) and in cultured, activated human peripheral blood–derived lymphocytes. No responses were seen in human neutrophils, monocytes, or Epstein-Barr virus–transformed B lymphoblastoid cell lines. rHuMig was chemotactic for TIL by a modified Boyden chamber assay but rHuMig was not chemotactic for neutrophils or monocytes. The CHO cell lines, IFN-γ–treated human peripheral-blood monocytes, and IFN-γ–treated cells of the human monocytic cell line THP-1 all secreted multiple and identical HuMig species as revealed by SDS-PAGE. Using the CHO-derived rHuMig, we have shown that the species' heterogeneity is due to proteolytic cleavage at basic carboxy-terminal residues, and that the proteolysis occurs before and not after rHuMig secretion by the CHO cells. The major species of secreted rHuMig ranged from 78 to 103 amino acids in length, the latter corresponding to the full-length secreted protein predicted from the HuMig cDNA. Carboxy-terminal–truncated forms of rHuMig were of lower specific activity compared to full-length rHuMig in the calcium flux assay, and the truncated species did not block the activity of the full-length species. It is likely that HuMig plays a role in T cell trafficking and perhaps in other aspects of the physiology of activated T cells.

Chemokines are members of a family of small, inducible, and secreted proteins. The chemokines are active as chemotactic factors and growth regulators, and exert their effects through seven transmembrane-domain G-protein–coupled receptors (1, 2). With the exception of the recently described chemokinelike factor lymphotactin (3), the chemokines contain four invariant cysteine residues and can be divided into two subfamilies. In the α or CXC subfamily, whose genes are found in a cluster on human chromosome 4, a single amino acid separates invariant cysteines 1 and 2. In the β or CC subfamily, whose genes are clustered on human chromosome 17, invariant cysteines 1 and 2 are adjacent. The CXC chemokines can be subdivided further based on the presence or absence of an NH_2-terminal region sequence, ELR, that is important for binding to the IL-8 receptors on the surfaces of neutrophils (4, 5). ELR-containing chemokines such as IL-8 function as chemotactic factors for neutrophils. The CC chemokines are chemoattractants for a variety of cells, such as monocytes, lymphocytes, basophils, eosinophils, and neutrophils (6–9). The chemokines are likely key components in conferring specificity on a number of the steps necessary for the selective trafficking of distinct populations of leukocytes and subpopulations of lymphocytes (10).

The activities of the chemokines are not limited to chemotaxis, and the chemokines can act on cells other than peripheral blood leukocytes. For example, the chemokines have been shown to have effects, primarily inhibitory, on the proliferation of myeloid progenitor cells (11, 12); the CC chemokines are active in stimulating exocytosis in hu-

Portions of this work were presented in abstract form at the Clinical Research Meeting of the American Federation for Clinical Research, 29 April–2 May 1994, Baltimore, MD, and at the Experimental Biology 95 meeting, 9–13 April 1995, Atlanta, GA.

 J. Exp. Med. © The Rockefeller University Press • 0022-1007/95/11/1301/14 $2.00
Volume 182 November 1995 1301–1314

man basophils (13); the CXC chemokine IL-8 is an angiogenic factor (14); and other CXC chemokines, platelet factor 4 (15) and IP-10 (16), can inhibit angiogenesis.

Differential screening of a cDNA library from lymphokine-activated macrophages led to the identification of a CXC chemokine, Mig (17). The *mig* gene is induced in mouse and human monocytes/macrophages specifically in response to IFN-γ (17, 18). Mig, like platelet factor 4, IP-10, stromal cell-derived factor (SDF)[1]-1α and SDF-1β (19), is a CXC chemokine lacking the ELR sequence. We describe here the purification of recombinant human Mig (rHuMig) from rHuMig-overexpressing Chinese hamster ovary (CHO) cells and we report the initial biochemical and functional characterization of the HuMig chemokine.

Materials and Methods

Expression of rHuMig in Escherichia coli. The HuMig cDNA (18) was cleaved with NlaIV and PstI to give a 664-bp fragment that encoded the predicted HuMig protein minus the signal peptide, including residues 23–125 of the HuMig open reading frame. After making the PstI end blunt using T4 DNA polymerase, BamHI linkers were added and the fragment was inserted into the BamHI site of the pET-3b vector (20) 3′ to a promoter for the T7 RNA polymerase. The resulting plasmid was predicted to give rise to an mRNA encoding a fusion protein with the NH_2-terminal 11 amino acids of the T7 bacteriophage gene *10* protein followed by three additional residues (RDP) and followed in turn by HuMig residues 23–125, consisting of the entire predicted, secreted HuMig protein (18). The gene *10* protein/HuMig fusion protein was produced in *E. coli* strain BL21 (DE3) as described by Studier et al. (20).

Expression of rHuMig in CHO Cells. Using PstI, a 785-bp fragment containing the entire coding sequence of HuMig was excised from the pBluescript SK-phagemid (Stratagene, La Jolla, CA) that contained HuMig cDNA (18). The termini were made blunt using T4 DNA polymerase and XhoI linkers were added, and the fragment was inserted into the XhoI site of pMSXND (21), 3′ to a mouse genomic fragment containing the metallothionein I promoter and 5′ to elements from the SV40 genome, including the small t antigen intron and the early region polyadenylylation sequence. pMSXND contains a mouse dihydrofolate reductase cDNA 3′ to the early promoter of SV40 and a neomycin resistance gene 3′ to a thymidine kinase promoter. CHO cells were proline auxotrophs (21) and were a kind gift from Se-Jin Lee, Johns Hopkins University. pMSXND DNA, containing the HuMig cDNA fragment in either the sense or the antisense orientation with respect to the metallothionein I promoter, was made linear by digestion with PvuI and was used to transfect CHO cells by the lipofectin method according to the manufacturer's protocol (GIBCO/BRL, Life Technologies, Gaithersburg, MD). Cells were grown in 400 μg/ml G418 (GIBCO/BRL, Life Technologies) to eliminate nontransfected cells, followed by growth without G418 but with 0.2 μM methotrexate (Sigma Chemical Co., St. Louis, MO) in MEM supplemented with 11.5 μg/ml proline and 10% dialyzed FCS (Sigma Chemical Co.). Methotrexate-resistant colonies were picked and analyzed for production of rHuMig by growing the cells in 100 nM cadmium sulfate, and subjecting supernatants to SDS-PAGE (22) followed by immunoblotting as described below. Cell line CHO/H9 was derived from cells transfected with DNA having the HuMig cDNA in the sense orientation. Cell line CHO/R5 was derived from cells transfected with DNA containing the HuMig cDNA in the antisense orientation. The CHO cell lines were not single-cell cloned.

For collecting supernatants for protein purification, the rHuMig overexpressing CHO cells were cultured in MEM-α (GIBCO/ BRL, Life Technologies), supplemented with 10% dialyzed FCS, 2 mM glutamine, and 0.2 μM methotrexate. When the cells became confluent, the culture medium was removed and replaced with serum-free MEM-α with 100 nM cadmium sulfate. After 12–24 h, the medium was discarded and fresh serum-free medium with cadmium was added. The harvesting and refeeding were done each 24 h and continued for 7 d and the supernatant from day 2 to day 7 was used as starting material for the purification of rHuMig.

Production of HuMig Antisera. The gene *10* protein/HuMig fusion protein expressed in bacteria was used to raise rabbit antisera JH49 and JH50. Bacterial lysates containing the gene *10*/HuMig fusion protein were separated by SDS-PAGE under reducing conditions. The fusion protein was visualized using 0.05% Coomassie brilliant blue, the band excised, and the gel lyophilized and pulverized for injection. New Zealand White rabbits were injected subcutaneously with material containing 100–200 μg of protein initially in complete, and subsequently in incomplete Freund's adjuvant, approximately once per month over 16 mo with regular bleeds.

Antisera JH49 and JH50 were used for immunoblotting. These antisera, raised against denatured rHuMig, were not efficient in immunoprecipitating HuMig, particularly the low-kD HuMig species (data not shown).

To raise antisera 5092, a rabbit was injected with 100 μg of the rHuMig high-kD species that had been purified from the overexpressing CHO/H9 cell line, and the rabbit was boosted with 60–100 μg of the rHuMig high-kD species per month over 3 mo. Antiserum 5092 was used successfully for immunoprecipitating the various forms of HuMig as described below.

IgG was purified from rabbit serum using protein A–activated Acti-Disk cartridges (FMC Bioproducts, Rockland, ME) according to the manufacturer's protocol.

SDS-PAGE, Silver Staining, and Immunoblotting. In general, samples were analyzed under reducing conditions using Tricine-SDS-PAGE and a 10–20% gradient gel (Jule Biotechnologies Inc., New Haven, CT) according to the method of Schagger and Von Jagow (23). For the determination of apparent molecular weights, a Tris-glycine-SDS, 15% acrylamide gel was used according to Laemmli (22). For immunoblotting, the proteins were electrotransferred to nitrocellulose membranes (Schleicher and Schuell Inc., Keene, NH) using a solution of 10 mM sodium bicarbonate, 3 mM sodium carbonate, pH 9.9/methanol of 8:2, in a TransBlot apparatus (Bio-Rad Laboratories, Hercules, CA) at 45 V for 7 h in the cold. The membranes were blocked with 50 mM Tris/HCl, pH 7.5, 150 mM NaCl, 0.1% Tween-20, and 10% milk (1–2% fat) and all incubations and washes were done in the presence of the blocking solution. Blots were incubated with rabbit anti-HuMig serum JH50 at a 1:1,000 dilution, washed, and incubated with horseradish peroxidase–conjugated goat anti–

[1]*Abbreviations used in this paper:* CHO, Chinese hamster ovary; CM, carboxymethyl; MCP, monocyte chemotactic protein; MIP, macrophage inflammatory protein; PVDF, polyvinylidene difluoride; rHuMig, recombinant human Mig; SDF, stromal cell-derived factor; TIL, tumor-infiltrating lymphocyte.

rabbit IgG (Jackson ImmunoResearch Laboratories, Inc., West Grove, PA) at a 1:5,000 dilution, washed again, and visualized by chemiluminescence using the ECL reagents according to the manufacturer's protocol (Amersham Corp., Arlington Heights, IL). The markers used routinely for the immunoblots were the prestained protein molecular weight standards from GIBCO/BRL, Life Technologies. The high-kD species of HuMig (see below) reproducibly comigrated with both prestained lysozyme as well as with lysozyme that had not been prestained. For this reason, the position of the prestained lysozyme on the immunoblots is designated as 14.3 kD, lysozyme's reported molecular mass, without regard to changes in the mobility of the marker due to prestaining. Silver staining of proteins was performed according to the method of Blum (24). The markers used for silver-stained gels and for the determinations of apparent molecular weights were the Mark 12 wide-range proteins standards from Novel Experimental Technology (San Diego, CA).

Analysis of HuMig Production by THP-1 Cells and by Peripheral Blood Monocytes. THP-1 cells, derived from a human histiocytic lymphoma, were obtained from the American Type Culture Collection, Rockville, MD. Human peripheral blood monocytes were collected from normal donors by elutriation by the Department of Transfusion Medicine, Clinical Center, National Institutes of Health. THP-1 cells and monocytes were cultured routinely in RPMI 1640 with 10% FCS. For analysis of HuMig production by the THP-1 cell line, cells were incubated at a density of 10^6 cells/ml for 30 h without or with 2,000 U/ml IFN-γ. For analysis of HuMig production by peripheral blood monocytes, cells were incubated at a density of 10^6 cells/ml for 48 h without or with 2,000 U/ml IFN-γ. Protease inhibitors leupeptin 2 μg/ml, EDTA 1 mM, PMSF 0.5 mM, aprotinin 2 μg/ml, bestatin 10 μg/ml, calpain inhibitor 17 μg/ml, E-64 1 μg/ml, and pepstatin 0.7 μg/ml (Boehringer Mannheim Corp., Indianapolis, IN) were added to the cell supernatants before the samples were concentrated for analysis. Anti-HuMig serum 5092 and protein A–Sepharose (Pharmacia LKB Biotechnology, Piscataway, NJ) were used for immunoprecipitation. The precipitates were analyzed by Tricine-SDS-PAGE and immunoblotting as described above.

Purification of rHuMig Proteins. (*a*) Purification of high-kD proteins. The culture supernatants from rHuMig-overexpressing CHO/H9 cells were collected as described above and made 50 mM Tris/HCl pH 7.5 and 0.5 mM EDTA. 8–10 liters of supernatant were loaded on a carboxymethyl (CM)-cellulose column (MetaChem Technologies Inc., Torrance, CA) mounted on a ConSep LC100 liquid chromatograph (Millipore Co., Milford, MA) and the bound proteins were eluted with a linear gradient of 0.025–1 M NaCl in 50 mM Tris/HCl pH 7.5, 0.5 mM EDTA. The high-kD rHuMig species eluted as a single asymmetrical peak at ~0.5 M NaCl. Fractions containing rHuMig were identified by immunoblotting and peak fractions were pooled, concentrated using the Centriprep-3 device (Amicon Inc., Beverly, MA), and subjected to reversed phase HPLC on a 46 cm × 15 cm C18 column (Vydac, Hesperia, CA). The rHuMig species were eluted using a gradient of 15–40% acetonitrile in 0.05% TFA over 60 min at a flow rate of 1 ml/min on a liquid chromatograph (model 1050; Hewlett-Packard Co., Palo Alto, CA). The column eluate was monitored at 280 nm, 205 nm, and, for reference, at 450 nm. The high-kD rHuMig species eluted at ~44 min. (*b*) Purification of low-kD species. The flow-through from the CM-cellulose column as described above was collected, concentrated 20–40-fold using a spiral wound CH2 apparatus (Amicon Inc., Beverly, MA), and the concentrate was dialyzed against 25 mM Tris/HCl pH 7.5, 0.5 mM EDTA, and 25 mM NaCl. The dialyzed sample was reapplied to the CM-cellulose column and the bound proteins were eluted with a linear gradient of 0.025–1 M NaCl in 25 mM Tris/HCl, pH 7.5, 0.5 mM EDTA. The ability of the low-kD rHuMig to bind to the CM-cellulose column after dialysis was presumably due to the lower ionic strength of the dialysis buffer (~0.02) as compared with the ionic strength of the initial CHO cell supernatants (~0.17). The low-kD rHuMig species eluted as a single asymmetrical peak at ~0.4 M NaCl. Fractions containing rHuMig low-kD species were identified by immunoblotting, pooled, and concentrated using Centriprep-3 and Centricon-3 devices. 150–200-μl samples were chromatographed on a 1 cm × 30 cm Superose 12 HR column (Pharmacia LKB Biotechnology) equilibrated with 25 mM Tris/HCl, pH 7.5, 0.15 M NaCl and 0.5 mM EDTA. The rHuMig-containing fractions were pooled, concentrated, applied to a 46 cm × 15 cm C18 column, and eluted using a 60-min linear gradient of 23–30% acetonitrile in 0.05% TFA at a flow rate of 1 ml/min. The low-kD rHuMig species eluted between 32 and 43 min.

HPLC fractions with purified rHuMig were evaporated to dryness and the protein was resuspended in 10 mM Tris/HCl, pH 7.5, at ~0.6 g/ml and stored at −70°C.

rHuMig protein concentrations were determined by the bicinchoninic acid method (25) according to the supplier's protocol (Pierce Chemical Co., Rockfield, IL) using BSA as the standard.

NH_2-Terminal Amino Acid Analysis. The purified rHuMig species were subjected to Tricine-SDS-PAGE and transferred to a polyvinylidene difluoride (PVDF) membrane (Trans-Blot; Bio-Rad Laboratories). The membrane was stained with Ponceau S and destained with 0.1% acetic acid. The protein bands were excised and the membrane was washed exhaustively with deionized water. The PVDF membrane was placed in the Blott™ reaction cartridge of a protein sequencer (model 470A; Applied Biosystems Inc., Foster City, CA) and subjected to automated Edman degradation using the manufacturer's recommended cycles for gas phase delivery of TFA. The resultant phenylthiohydantoin amino acid fractions were manually interpreted using an on-line HPLC (model 120A; Applied Biosystems Inc.) and (CR4; Shimadzu Corp., Tokyo, Japan) integrator. The protein sequencing was done by the Harvard Microbiochemistry Facility.

Electrospray Ionization Mass Spectrometry. For mass determinations, purified rHuMig species were prepared by dissolving dried HPLC fractions in 30 μl of methanol/water (1:1). Mass spectra were recorded on a triple quadrupole mass spectrometer (TSQ-700; Finnigan-MAT, San Jose, CA) equipped with an electrospray ion source. Fractions were brought to a concentration of 50% methanol/0.5% acetic acid and directly infused at a flow rate of 1 μl/min. The electrospray needle was operated at a voltage differential of −3 to −4 keV. Spectra were recorded by scanning the m/z range of 400–2,000 in 3 s and averaging 16–32 scans. The electrospray ionization mass spectrometry was performed by the Harvard Microbiochemistry Facility.

Tumor-infiltrating Lymphocytes (TIL). The TIL were prepared from human melanomas as described (26). The F9 and B10 lines of TIL were maintained routinely in RPMI 1640 with 10% FCS containing 500 U/ml IL-2 (Cetus Oncology Corp., Emeryville, CA) or 100 U/ml IL-2, respectively. The TIL were periodically stimulated with PHA plus irradiated allogeneic PBMC. For stimulation, buffy coats collected from normal donors by the Department of Transfusion Medicine, Clinical Center, National Institutes of Health, were treated with 5,000 rad. The PBMC were purified by Ficoll-Hypaque (Pharmacia LKB Biotechnology Inc.)

banding, and then washed and resuspended at 10^7 cells/ml in routine culture medium with 250 ng/ml PHA (Murex, Dartford, UK). The TIL were suspended at 2×10^6 cells/ml and equal volumes of the suspensions of PBMC and TIL were mixed and cultured in 24-well culture plates (Costar Corp., Cambridge, MA) with 1 ml/well. After 3–4 d, 1 ml routine culture medium without PHA was added to each well. After 2–3 additional d, the cells were transferred to flasks at a density of 10^6 cells/ml.

Activation of PBL. The elutriated PBL and monocytes were collected from normal donors by the Department of Transfusion Medicine, Clinical Center, National Institutes of Health. The PBL were purified further by banding on Ficoll-Hypaque. The purified lymphocytes were washed with Dulbecco's PBS and resuspended in RPMI 1640 supplemented with 10% FCS, 100 U/ml penicillin, 100 μg/ml of streptomycin, and 5 μg/ml PHA. The elutriated syngeneic monocytes were treated with 5,000 rad, washed with Dulbecco's PBS, and resuspended in the same medium used for the PBL. Equal volumes of the lymphocyte suspension (2×10^6 cells/ml) and the monocyte suspension (10^6 cells/ml) were mixed and cultured in 96-well round-bottomed plates for 4 d (27).

Measurements of Calcium Flux. Calcium flux assays were done according to the method of Grynkiewicz (28). For calcium measurements, recombinant IL-8 was obtained from Biosource (Camarillo, CA), and recombinant human MCP-1 and IP-10 were obtained from PeproTech (Rocky Hill, NJ). Neutrophils were prepared as described (29). B lymphoblastoid cell lines 81EBV, LAZ 509, and 414EBV were the kind gift of Robert Siliciano, Johns Hopkins University, and the cells were grown in RPMI 1640 with 10% FCS. TIL and PBL and monocytes were obtained and cultured as described above. Cells were suspended at a density of 2×10^6 cells/ml in HBSS containing 1.3 mM $CaCl_2$, 10 mM Hepes, pH 7.3, and 1% FCS. The cells were loaded with 2 μM Fura-2, AM (Molecular Probes Inc., Eugene, OR) for 1 h at 30°C with occasional shaking. Loaded cells were washed twice by centrifugation and resuspended at a concentration of 10^6 cells/ml. The cell suspension was brought to 37°C and immediately before each assay 10^6 cells were collected by centrifugation, resuspended in 2 ml HBSS/Hepes/FCS, and added to a cuvette in a temperature-controlled (37°C) holder with continuous stirring. Calcium measurements were done using a ratio fluorescence spectrometer (model RF-M2001; Photon Technology International, South Brunswick, NJ). Excitation was alternately at 340 and 380 nm with emission measured at 510 nm. Using an integration time of 0.5 s the ratios of the signals obtained at the two excitation wavelengths were plotted as a function of time.

Measurements of Chemotaxis. Assays for lymphocyte chemotaxis using the B10 TIL were done by a modified Boyden chamber procedure using an MBC 96 microtiter plate chamber, 5-μm pore size polyvinylpyrrolidone-free polycarbonate membranes (Neuro Probe, Cabin John, MD), and customized 96-microwell viewplates (Polyfiltronics Group Inc., Rockland, MA). The B10 TIL were preincubated at 5×10^6 cells/ml in RPMI/1% FCS containing 10 μM calcein, AM (Molecular Probes Inc.), at 37°C for 1 h. Dye-loaded cells were pelleted, washed, and resuspended in RPMI/1% FCS at 10^7 cells/ml. Samples of RPMI/1% FCS without or with rHuMig were prewarmed to 37°C and ~400 μl was placed in each microwell, the microwells forming the lower chambers. Each test sample was loaded into three adjacent microwells. After assembling the apparatus, 50 μl of the cell suspension was added to each upper well and the apparatus was incubated at 37°C in 5% CO_2 for 3 h. After disassembling the apparatus and removing the filter, the microtiter plate was centrifuged at 400 *g* at 4°C for 3 min and the medium was aspirated from the microwells. The cells were washed in HBSS with repeat centrifugation and the cells were resuspended and lysed in HBSS with 0.5% SDS. Fluorescence was measured using a microtiter plate reader (Titertek Fluoroskan II; Flow Laboratories, Lugano, Switzerland) with excitation at 485 and emission read at 538 nm. Serial dilutions of the cell suspension had been added in place of test samples to one row of microwells for establishing a standard curve relating fluorescence intensity to cell number and values of fluorescence intensity were converted into numbers of cells migrating by reference to the standard curve. The relationship between cell number and fluorescence intensity was linear over the range of the experimental values that were obtained.

Assays for chemotaxis of neutrophils and monocytes were done using a 48-well microchemotaxis chamber (Neuro Probe) as described (30). Neutrophils and monocytes were obtained as described above. For testing neutrophils, cells were used at a concentration of 10^6/ml. The filter was polycarbonate, polyvinylpyrrolidone-free, with 3-μm pores (Costar Corp). For testing monocytes, cells were used at a concentration of 1.5×10^6/ml. The filter was polycarbonate, polyvinylpyrrolidone coated with 5-μm pores (Poretics Corp., Livermore, CA). Filters were analyzed by counting the cells in five high-power fields per well.

Results

Production of a CHO Cell Line Secreting rHuMig. CHO cells were transfected with the pMSXND plasmid into which had been inserted HuMig cDNA sequences, and rHuMig-secreting cell lines were derived by selection in methotrexate as detailed in Materials and Methods. CHO cells were chosen as a source of recombinant protein because they could be manipulated to yield lines secreting quantities of rHuMig far in excess of what could be obtained from a natural source (see below) and because conditioned medium could be harvested from CHO cells cultured without added protein, thereby simplifying rHuMig purification. In addition, CHO cells as compared with bacteria or cells of lower eukaryotes, could be expected to process HuMig similarly to human cells.

Transfection of CHO cells with pMSXND containing HuMig cDNA sequences in the sense orientation with respect to the mouse metallothionein I promoter yielded the CHO/H9 cell line. The CHO/R5 cell line was derived from cells transfected with pMSXND containing HuMig cDNA sequences in the antisense orientation. The CHO/R5 cell line served as a source of control conditioned medium lacking rHuMig.

As described in Materials and Methods, rabbit antisera JH49 and JH50 were raised against HuMig protein sequences expressed in *E. coli* and rabbit antiserum 5092 was raised against rHuMig high-kD species purified from the CHO/H9 cell line (see below).

As shown in Fig. 1, the cell line CHO/H9 secreted a collection of anti–HuMig-reactive polypeptides. As expected, no rHuMig protein was produced by the parent, nontransfected CHO cells, or by the methotrexate-resistant CHO/R5 cells that had been transfected with pMSXND containing HuMig cDNA sequences in the antisense orientation.

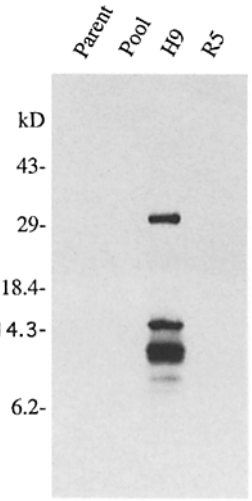

Figure 1. Production of rHuMig protein by transfected CHO cells. Culture supernatant was prepared from the parent CHO cell line, from the pool of G418-resistant CHO cells after transfection with the pMSXND/HuMig plasmid, and from the methotrexate-resistant cell lines CHO/H9 and CHO/R5, the former derived from cells transfected with the pMSXND plasmid containing the HuMig cDNA in the sense orientation and the latter with the HuMig cDNA in the antisense orientation. 24-h supernatants were collected from flasks containing confluent CHO cells and 50 μl of the conditioned medium (containing ~1.5 μg total protein) was loaded per lane and analyzed by Tricine-SDS-PAGE and immunoblotting using anti-HuMig serum JH50. The positions of prestained protein molecular weight standards (GIBCO/BRL Life Technologies) are shown.

The initial pool of transfected, G418-resistant CHO cells, while expressing detectable levels of HuMig-hybridizing RNA (not shown) did not secrete sufficient amounts of protein for detection by Western blot. For estimating relative molecular masses the CHO/H9 supernatant was analyzed by Tris-glycine SDS-PAGE using a 15% gel (not shown) that revealed predicted molecular masses for the rHuMig species of ~8–36 kD.

While the rHuMig species running at the 14.3-kD marker and below had predicted molecular masses in the 11,725-M_r range as predicted for the secreted protein on the basis of the HuMig cDNA sequence, it was puzzling that the CHO cells produced a reduced and denatured rHuMig species running as a discrete band between the 29- and 43-kD markers (Fig. 1). Moreover, production of this species was not unique to the CHO/H9 cell line but was found in supernatants from 12 other transfected, methotrexate-resistant, rHuMig-secreting CHO cell lines (data not shown). Northern blot analysis of the HuMig RNA species produced by the CHO/H9 cells revealed evidence for alternative splicing (data not shown). Northern blot analysis using oligonucleotide probes and PCR analysis of cDNA did not suggest the presence in the CHO/H9 cells of any HuMig RNA species where the HuMig stop codon had been deleted (data not shown). Nonetheless, we considered whether there might be a minor RNA species where splicing had in fact deleted the HuMig stop codon and fused Mig sequences with those of the SV40 large T antigen from the pMSXND vector. We investigated this possibility by probing a Western blot of supernatants of the rHuMig-producing CHO cells with mAb KT3, whose epitope is in the carboxy-terminal residues of the SV40 large T antigen (31), and found that, in fact, the low mobility species that was immunoreactive with anti-HuMig antibodies was likewise recognized by antibody KT3, while none of the 8–14.3-kD rHuMig species reacted with KT3 and no KT3-reactive species were present in supernatants from control CHO cells (data not shown). This HuMig/large T antigen fusion protein was not investigated further.

Comparison of HuMig Secreted by CHO Cells, Human Peripheral Blood Monocytes, and THP-1 Monocytic Cells. To compare the CHO-derived rHuMig and HuMig produced by human cells, monocytes, purified from peripheral blood by elutriation, and cells of the THP-1 histiocytic lymphoma line, were treated with IFN-γ and the cell supernatants were analyzed by immunoprecipitation followed by Western blot analysis. Supernatant from CHO/H9 cells was added to supernatant from control peripheral blood monocytes, or control THP-1 cells, and the mixtures were analyzed in parallel with the samples from the IFN-γ–treated cells. Fig. 2 shows that after treatment with IFN-γ, both peripheral blood monocytes and THP-1 cells secreted a collection of HuMig polypeptides whose mobilities were identical to those of species produced by the CHO cells. For this analysis, supernatants from IFN-γ–treated peripheral blood monocytes and THP-1 cells were concentrated 40-fold before SDS-PAGE. In Fig. 2, in light of the data presented below, we have divided the HuMig species into two groups, labeled high- and low-kD, and we will refer to these HuMig species as high- and low-kD in the remainder of the paper.

Analysis of the Basis for the HuMig Species of Differing Mobilities. The production of HuMig polypeptides of differing mobilities was most likely due to posttranslational modification, either augmentation of the mass of the polypeptide by glycosylation, and/or proteolytic cleavage of the full-length protein. The predicted HuMig protein lacks the sequence for N-linked glycosylation, and in other experiments not shown, digestion of rHuMig with peptide-*N*-glycosidase F or with *O*-glycanase failed to demonstrate

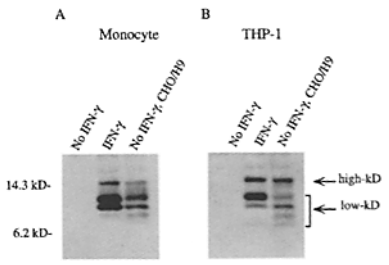

Figure 2. HuMig produced by IFN-γ–stimulated peripheral blood monocytes and THP-1 cells, compared with rHuMig produced by CHO cells. Peripheral blood monocytes were cultured at a density of 10^6 cells/ml for 48 h without or with 2,000 U/ml IFN-γ (*A*). THP-1 cells were cultured at a density of 10^6 cells/ml for 30 h without or with 2,000 U/ml IFN-γ (*B*). 40 ml of culture supernatant from monocytes and 30 ml of culture supernatant froms THP-1 cells were collected. Before processing for analysis, conditioned medium from the rHuMig-producing cell line CHO/H9 was added to a sample taken from monocytes and from THP-1 cells incubated without IFN-γ. 1 ml of CHO/H9-conditioned medium was added to the monocyte sample, and 0.75 ml was added to the THP-1 sample. After collection of the supernatants, protease inhibitors were added and the samples were concentrated, subjected to immunoprecipitation using anti-HuMig serum 5092, and analyzed by Tricine-SDS-PAGE and immunoblotting. The positions of prestained markers are designated on the left. The high- and low-kD species of HuMig are indicated on the right (see text).

any N-linked or O-linked sugar. Experiments were done to determine whether proteolysis was responsible for generating the multiple rHuMig species and if so, whether proteolytic processing occurred before or after the secretion of rHuMig from the cell.

Supernatants were harvested from CHO/H9 cells and incubated at 37°C, and analysis of serial samples showed no change in the pattern of rHuMig immunoreactive species over 8 h, i.e., no conversion of high- to low-kD forms (data not shown). Next, medium was harvested from CHO/H9 cells that had been incubated with or without protease inhibitors for various times from 1 to 24 h, and the media from the 1–12-h time points were concentrated appropriately so as to normalize the rHuMig concentrations among the samples. Western blot analysis of rHuMig produced by CHO/H9 cells incubated without protease inhibitors, as shown in Fig. 3, revealed that the pattern of rHuMig species did not change significantly over time, i.e., there was no evidence of processing occurring after secretion of the protein into the medium. In the presence of protease inhibitors, only the high-kD species accumulated, consistent with our presumption that the low-kD species were derived from the high-kD species by proteolytic processing. The effect of the protease inhibitors is consistent with proteolysis occurring before secretion since it has been shown that these agents can inhibit intracellular proteolysis (32–34). The relationships among the various rHuMig species were clarified further after the proteins' purifications.

Purification of rHuMig. CHO/H9 cells were grown in protein-free medium and culture supernatant was used as the starting material for the purification of rHuMig. As described in Materials and Methods CM-cellulose chromatography separated rHuMig into high- and low-kD species. The high-kD rHuMig species was purified additionally by reversed phase chromatography. The low-kD rHuMig species were purified by repeat application to CM-cellulose, followed by size-exclusion and reversed phase chromatography.

Fig. 4 shows separation by SDS-PAGE followed by silver staining or immunoblotting of the CHO/H9 supernatant and of the purified rHuMig species. Minor bands running above the 14.4-kD marker, such as those evident with silver staining in Fig. 4, were seen routinely with SDS-PAGE analysis of large amounts of purified rHuMig. These minor species were immunoreactive (discernible but not seen easily on the exposure of the immunoblot in Fig. 4), and their mobilities varied along with the mobilities of the major rHuMig species (see Fig. 5), so that we presumed that these species represented aggregates of the major species, formed during the processing for SDS-PAGE.

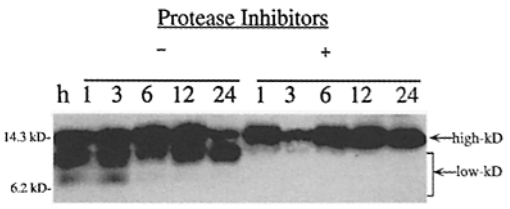

Figure 3. Effect of protease inhibitors on the processing of rHuMig. Confluent CHO/H9 cells were grown in serum-free medium in the absence of protease inhibitors or in the presence of the protease inhibitors aprotinin (0.3 μM), leupeptin (50 μM), and *N*-1-tosylamide-2-phenylethylchloromethyl ketone (TPCK) (25 μM). Supernatants were collected at the times indicated. The 1-, 3-, 6-, and 12-h supernatants were concentrated 24-, 8-, 4-, and 2-fold respectively. 50 μl of each sample was analyzed by Tricine-SDS-PAGE followed by immunoblotting using anti-HuMig serum JH50. The positions of prestained markers are designated on the left. The high- and low-kD species of rHuMig are indicated.

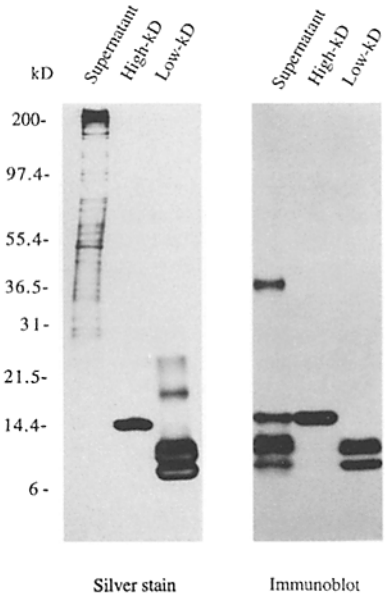

Figure 4. High- and low-kD species of rHuMig purified from CHO/H9 cells. (*Left*) Crude supernatant from CHO/H9 cells, containing 5 μg of total protein and samples of purified high- and low-kD rHuMig species containing 1 and 2 μg of protein, respectively, were analyzed by Tricine-SDS-PAGE and silver staining. The positions of protein standards (Novel Experimental Technology) are noted on the left. (*Right*) Using the same samples as used for the left panel, crude supernatant from CHO/H9 cells containing 3 μg of total protein, and aliquots of purified high- and low-kD rHuMig species containing 5 ng of protein each were analyzed by Tricine-SDS-PAGE followed by immunoblotting using anti-HuMig serum JH50.

NH_2-Terminal and Mass Determinations of rHuMig Species. Four fractions of HPLC-purified rHuMig, containing rHuMig polypeptides of varying mobilities, were subjected to SDS-PAGE and the proteins transferred to a PVDF membrane. NH_2-terminal analysis of the rHuMig polypeptides revealed a single predominant sequence irrespective of the species' mobilities, namely TPVVR, the HuMig NH_2-terminal sequence that had been predicted (18) based on the empirically derived rules for signal-peptide cleavage.

Analysis of similar HPLC fractions by electrospray ionization mass spectrometry revealed species with masses ranging from 11,723 to 8,464. The predicted COOH-terminal residues of the major species are indicated in Fig. 5. In general, cleavage has left a basic COOH-terminal residue typical of the products of many serine proteases. In addition, the mass analysis confirmed the absence of glycosylation. The differences in binding properties of the high-

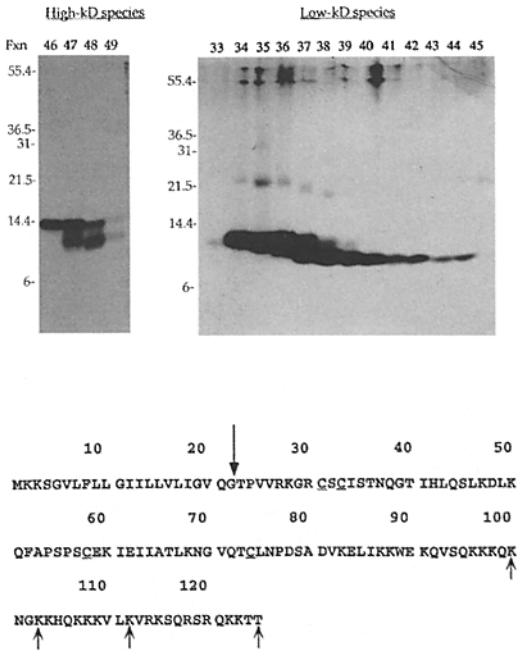

Figure 5. Reversed phase chromatography of high- and low-kD rHuMig species showing results of NH_2-terminal analysis and showing the predicted COOH termini of selected fractions. The high- and low-kD species of rHuMig obtained from 10 liters of conditioned medium from CHO/H9 cells, were subjected to reversed phase chromatography on a Vydak C18 column as described in Materials and Methods. 10 μl of each HPLC fraction was analyzed by Tricine-SDS-PAGE followed by silver staining, as shown in the upper panel. rHuMig species from high-kD fraction 46 and low-kD fractions, 34, 37, and 39 were transferred to a PVDF membrane and the NH_2-terminal sequences were determined. Comparable fractions from another HPLC separation were analyzed by electrospray ionization mass spectrometry. The mass values were used for determining the rHuMig species' COOH termini. The predicted amino acid sequence of the unprocessed HuMig protein is indicated below with the site of cleavage of the signal peptide for rHuMig shown by the down-going arrow. The predicted COOH-terminal residues of the major rHuMig species are designated by the up-going arrows.

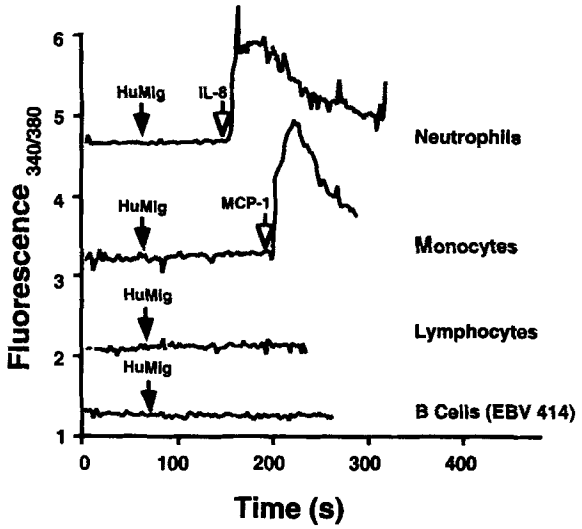

Figure 6. Failure of high-kD rHuMig to induce calcium fluxes in neutrophils, monocytes, PBL, or EBV-transformed B cells. At the times indicated by the solid arrows, high-kD rHuMig was added to 10^6 Fura-2, AM-loaded cells in 2 ml HBSS/Hepes/FCS to give a final concentration of rHuMig of 100 ng/ml. At the times indicated by the open arrows, 10 ng/ml rIL-8 was added to the neutrophils and 50 ng/ml of rMCP-1 was added to the monocytes. The cells were obtained and the fluorescence measurements were done as described in Materials and Methods. No responses to the purified high-kD rHuMig were seen for neutrophils from two donors in three experiments, for monocytes from two donors in two experiments, for freshly isolated PBL from two donors in two experiments, and for EBV-transformed B lymphoblastoid cell lines from three donors in two experiments.

and low-kD species for CM-cellulose as described above are understandable, given that the low-kD species are derived from the high-kD species by cleavage of basic COOH-terminal residues. The mass analysis established that HuMig species show anomalously decreased mobility when analyzed by Tricine-SDS-PAGE or by Tris-glycine-SDS-PAGE (not shown) with the 11,725-M_r species, for example, running at a mobility of ~14 kD. The basis for this anomalous behavior is unknown, but may relate to the highly basic character of the HuMig protein, and has been seen with other chemokines (35).

Demonstration that rHuMig Targets T Cells. The receptors for the chemokine family of cytokines are 7–transmembrane-domain proteins and, in general, binding of chemokines to their receptors leads to a transient rise in $[Ca^{2+}]_i$ (2). As shown in Fig. 6 rHuMig failed to cause a rise in $[Ca^{2+}]_i$ in neutrophils, monocytes, lymphocytes that had been freshly isolated from blood, or EBV-transformed B lymphoblastoid cells. Furthermore, 100 ng/ml of high-kD rHuMig failed to block an rIL-8–induced calcium flux in neutrophils or an rMCP-1–induced calcium flux in monocytes.

To limit the heterogeneity of the lymphocyte population being studied and because of the possibility that the responsiveness of lymphocytes to rHuMig might depend on the cells' state of activation, we evaluated the effect of rHuMig using TIL that had been derived from human melanomas (see Materials and Methods) and using a CTL clone specific for gp160 of HIV type I (36).

TIL lines F9 and B10 (see below) showed a rise in $[Ca^{2+}]_i$ in response to the purified high-kD rHuMig protein. The gp160-specific $CD4^+$ CTL clone F14.38 (36) also responded to rHuMig (not shown). Initial characterization of the F9 and B10 lines revealed that >97% of cells from both lines stained positive for CD3 and CD4 by FACS® analysis (data not shown). These TIL lines could be maintained in culture with intermittent restimulation (see Materials and Methods), and they were used in the studies shown below.

Experiments were done to demonstrate that the calcium response in TIL was due to rHuMig and not due to a contaminating protein present in amounts below the limits of detection of our analyses by physical methods. rHuMig peak fractions and adjacent fractions from the final reversed phase chromatography purification of the high-kD species were tested for their activities on the F9 TIL line. As shown in Fig. 7, the peak of activity corresponded to the rHuMig protein peak.

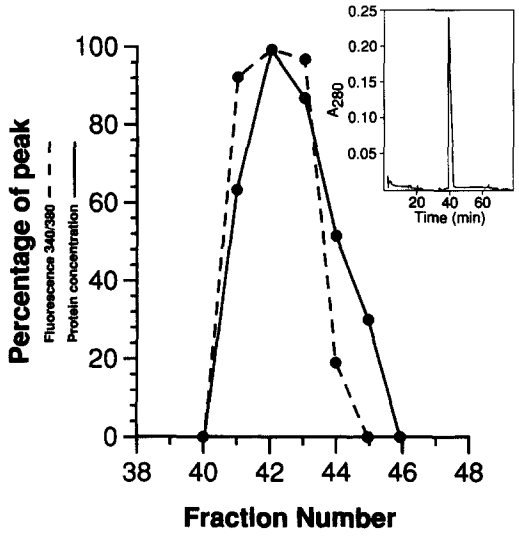

Figure 7. Reversed phase chromatography of rHuMig high-kD species showing coelution of rHuMig protein and the factor causing calcium flux in TIL. 160 μg of high-kD CM-cellulose–purified rHuMig was loaded on a Vydak C18 column. rHuMig was eluted using a gradient of increasing concentrations of acetonitrile and 1-ml fractions were collected. The HPLC chromatogram is shown as an inset. Fractions were assayed for the ability to cause a calcium flux in Fura-2, AM-loaded F9 TIL. Appropriate dilutions were made of fraction 42 to be within a dose-responsive range for measuring factor activity, and other fractions were diluted identically. Protein determinations were done on each fraction. Both the peak ratio of fluorescence intensities and the protein concentration for each fraction are expressed as a percentage of the maximum values.

Antisera JH49 and JH50, which had been raised against *E. coli*–derived rHuMig, could neutralize the activity of CHO/H9-derived rHuMig on TIL. Neutralization using IgG purified from one of the rabbits is shown in Fig. 8. Neutralization required preincubation of rHuMig with the anti-HuMig IgG. Neutralization was not due to any direct effect of the IgG on the TIL, since the lymphocytes responded to rHuMig added alone subsequent to the addition of the preincubated rHuMig–anti-rHuMig mixture.

Determination of the Dose Response of TIL to High-kD rHuMig and to rHuMig with a Deleted Carboxy Terminus. Fig. 9 *A* demonstrates the dose response of the F9 TIL line to a preparation of the high-kD rHuMig consisting primarily of the full-length, 103–amino acid species, with an EC_{50} of ~3 ng/ml. In Fig. 9 *B* is shown the dose response using rHuMig with carboxy-terminal deletions, equivalent to the material seen in fraction 39 in Fig. 5 where the major rHuMig species was 78 amino acids in length. While this rHuMig fraction does have some activity, it is <1/300 the activity of the high-kD rHuMig. Fig. 9 *B* also shows that the carboxy terminal–deleted rHuMig, when added at 1,000 ng/ml still did not produce a maximal rise in $[Ca^{2+}]_i$, and 1,000 ng/ml of the terminal-deleted species attenuated, but failed to block completely the response to 3 ng/ml of the high-kD rHuMig. The failure of the low-kD rHuMig species to eliminate completely the response to the high-kD species does not suggest that the rHuMig species are working through different receptors or signaling pathways,

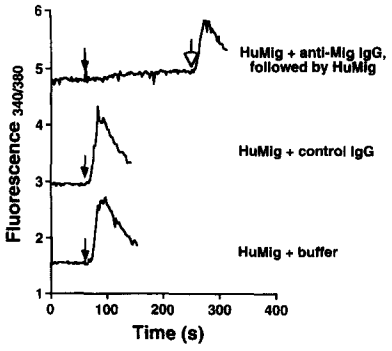

Figure 8. Neutralization of the factor stimulating a calcium flux in TIL using antibodies against rHuMig. 14 ng of high-kD rHuMig was preincubated for 3 h at 4°C in 50 μl of Dulbecco's PBS alone, or with 50 μg of IgG from a nonimmunized rabbit, or with 50 μg of IgG purified from anti-HuMig rabbit serum JH49. As indicated by the solid arrows, preincubated material was added to a cuvette containing 10^6 Fura-2, AM-loaded B10 TIL in 2 ml of HBSS/Hepes/FCS. The open arrow indicates the addition of 14 ng of high-kD rHuMig that had not been preincubated with IgG.

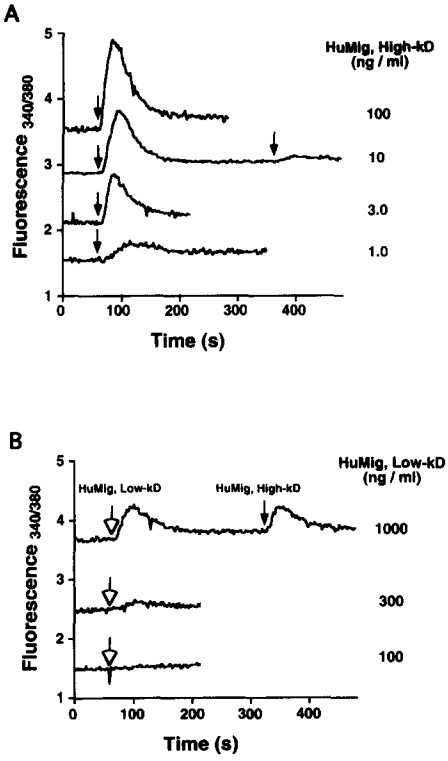

Figure 9. Calcium fluxes in TIL in response to varying concentrations of high- and low-kD rHuMig. (*A*) High-kD rHuMig was added to 10^6 Fura-2, AM-loaded F9 TIL in 2 ml of HBSS/Hepes/FCS when indicated by the arrows to give the final concentrations of high-kD rHuMig as noted on the right. After stimulation with 10 ng/ml rHuMig, a second, identical aliquot of rHuMig was added as indicated by the arrow at 360 s. (*B*) Low-kD rHuMig was added as in *A* to Fura-2, AM-loaded F9 TIL when indicated by the open arrows to give the final concentrations of low-kD rHuMig as noted on the right. After stimulation with 1,000 ng/ml of low-kD rHuMig, the cells were challenged with 3 ng/ml of the high-kD rHuMig as indicated by the solid arrow.

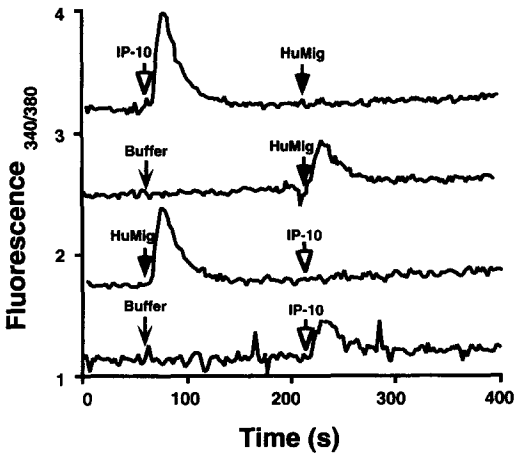

Figure 10. rIP-10–induced calcium flux in TIL. At the times indicated by the arrows chemokine or buffer alone was added to 10^6 Fura-2, AM-loaded B10 TIL in 2 ml of HBSS/Hepes/FCS. rIP-10 was added at 60 s at 200 ng/ml and at 210 s at 10 ng/ml. High-kD rHuMig was added at 60 s at 10 ng/ml and at 210 s at 2 ng/ml. For the bottom tracing several points that extended below the baseline were omitted for the sake of clarity.

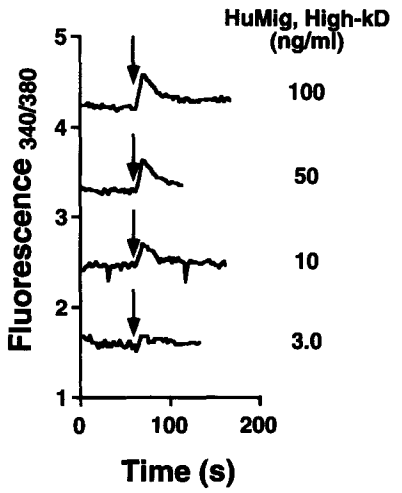

Figure 11. rHuMig-induced calcium fluxes in PBL that had been cultured and activated in vitro. Human PBL, purified from a normal donor by elutriation followed by banding on Ficoll, were incubated for 4 d in the presence of PHA and irradiated syngeneic monocytes. After loading with Fura-2, AM, 10^6 lymphocytes in 2 ml HBSS/Hepes/FCS were stimulated at the times indicated by the arrows with the concentrations of high-kD rHuMig as noted on the right.

since the response to the low-kD species was submaximal (see Fig. 9 *A*) and would therefore not be expected to prevent a response to a subsequent challenge.

Demonstration that TIL Also Respond to rIP-10. We were interested in determining whether rHuMig was the only chemokine capable of inducing a calcium flux in TIL. As discussed below, Mig shares features with IP-10 and since rIP-10 had been reported to be chemotactic for activated T cells (37), we tested the response of the TIL to rIP-10. As shown in Fig. 10, rIP-10, like rHuMig, caused a rise in $[Ca^{2+}]_i$ in the B10 TIL. To test rHuMig/rIP-10 cross-desensitization, concentrations of rHuMig and rIP-10 that produced maximal responses were chosen for the initial challenges and concentrations close to the EC_{50}'s were chosen for the second challenges. rIP-10 at 200 ng/ml blocked the response to a subsequent challenge with 2 ng/ml rHuMig and rHuMig at 10 ng/ml eliminated the response to a subsequent challenge with 10 ng/ml rIP-10, demonstrating cross-desensitization by rHuMig and rIP-10 in the B10 TIL.

Demonstration that PBL Can Respond to rHuMig. Because we were able to demonstrate a rise in $[Ca^{2+}]_i$ in TIL but not in freshly isolated PBL in response to rHuMig, we hypothesized that lymphocytes might need to be activated to respond to rHuMig. PBL were obtained from normal donors by elutriation followed by Ficoll-Hypaque discontinuous density gradient centrifugation and the lymphocytes were cultured for 4 d with PHA and irradiated syngeneic monocytes. Calcium fluxes in response to various concentrations of rHuMig are shown in Fig. 11. These data demonstrated that rHuMig-responsive cells could be detected in the PBL population after culture and activation in vitro. Lymphocytes were tested from a total of five donors and in four of the five the lymphocytes showed a rise in $[Ca^{2+}]_i$ in response to rHuMig. In general, the activated PBL required a higher concentration of rHuMig to detect a rise in $[Ca^{2+}]_i$ as compared with the TIL.

Demonstration that rHuMig Is Chemotactic for TIL. B10 TIL were loaded with the fluorescent vital dye calcein, AM, and we determined the TIL migration across a polycarbonate filter in response to rHuMig. Data from a representative experiment are displayed in Fig. 12. When 5×10^5 cells were placed in the upper chamber with 25 ng/ml of the high-kD rHuMig in the lower chamber, $\sim 1.4 \times 10^5$ cells migrated into the lower chamber over the background number of cells that migrated in the absence of rHuMig.

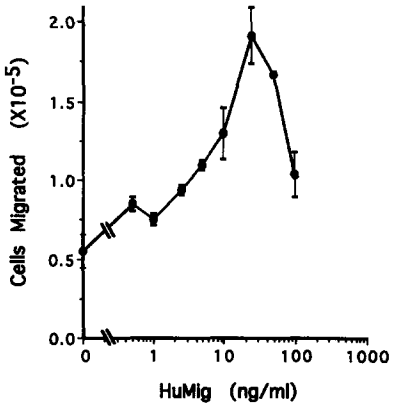

Figure 12. rHuMig-induced chemotaxis in TIL. Calcein AM-loaded B10 TIL were analyzed for their migration toward various concentrations of high-kD species of rHuMig using a modified Boyden chamber assay. 5×10^5 cells were added to the upper chambers and the numbers of cells migrating across the polycarbonate filter into the lower chamber are expressed as the means ± SE of triplicate samples from one representative experiment.

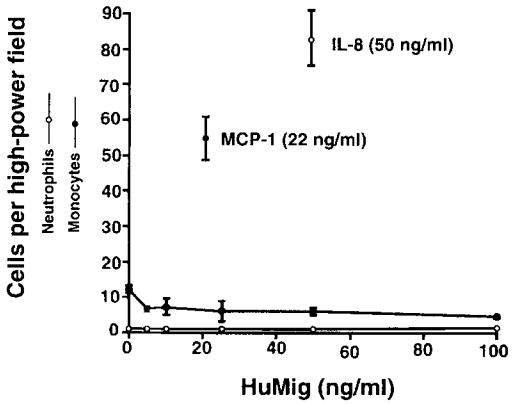

Figure 13. Failure of high-kD rHuMig to induce chemotaxis in neutrophils and monocytes. Assays were done using a 48-well microchemotaxis chamber and polycarbonate filters as described in Materials and Methods. Each concentration of rHuMig was tested in triplicate wells and for each of the wells the cells in five high-power fields were counted. The average number of cells per high-power field is plotted for each triplicate ± SE. Chemotactic responses of neutrophils to rIL-8 at the concentration indicated and of monocytes to rMCP-1 at the concentration indicated served as positive controls. A duplicate series of assays gave results identical to those shown here. Neutrophils and monocytes were each obtained from a single (but different) donor.

The decrease in cell migration seen at higher concentrations of rHuMig produces the "bell-shaped" dose-response curve characteristic for chemotactic factors. When rHuMig at a variety of concentrations was placed not in the lower chamber, but in the upper chamber together with the cells, there was no migration of B10 cells into the lower chamber over background levels (data not shown), demonstrating that rHuMig has true chemotactic activity for the B10 TIL. As shown in Fig. 13, using a standard microchemotaxis chamber (see Materials and Methods) the rHuMig high-kD species, when tested at 5–100 ng/ml, failed to elicit a chemotactic response in neutrophils or monocytes, consistent with the absence of rHuMig-induced calcium fluxes in these cells.

Discussion

We have demonstrated that HuMig is secreted as a collection of polypeptides that differ in their COOH termini as the result of proteolytic processing. We have shown that rHuMig targets activated T cells, causing both a rise in $[Ca^{2+}]_i$ and chemotaxis, and that rHuMig's ability to induce a signal is diminished by removal of COOH-terminal residues.

Both chemokines and nonchemokine cytokines have been demonstrated to cause T cells to chemotax (reviewed in 38). Studies of the actions of chemokines on lymphocytes have concentrated primarily on the CC or β chemokines, and these studies, while not always in agreement, have reported differential chemotactic effects for macrophage inflammatory protein (MIP)-1α versus MIP-1β (7–9) and for regulated upon activation in normal T cells expressed and secreted (RANTES) (6) on subpopulations of lymphocytes. It has been demonstrated recently that monocyte chemotactic protein (MCP)-1 is able to induce transendothelial lymphocyte migration (39).

While the CXC chemokines have been studied primarily for their effects on neutrophils, the CXC subfamily members IL-8 and IP-10 have been reported to be chemotactic for lymphocytes. Both IL-8 (40) and IP-10 (37) cause the migration of activated, but not of resting lymphocytes. The finding of lymphocyte chemotactic activity for IP-10 is of particular relevance to our work because Mig and IP-10 show a number of additional similarities. Along with platelet factor 4 and SDF-1 (19), IP-10 (37) and Mig (18) lack the ELR motif shared among the other CXC chemokines, a motif that is crucial for binding and activating the IL-8 receptors (4, 5). Computer-assisted sequence comparisons reveal that HuMig and IP-10 are somewhat more closely related to each other than they are to other chemokines (2). In both the mouse and the human, Mig and IP-10 are inducible in macrophages by IFN-γ (17, 18, 41, 42). Moreover, our data demonstrate that like rHuMig, rIP-10 can cause a calcium flux in TIL and that rHuMig and rIP-10 can each desensitize TIL to subsequent challenge with the other. The cross-desensitization data are consistent with rHuMig and rIP-10 binding to identical receptor(s). Cross-desensitization by two ligands does not establish, however, that their receptor(s) are shared. For example, the chemoattractants formylpeptide and C5a demonstrate cross-desensitization when tested on neutrophils despite their binding to separate hepta-helical receptors (43) and IL-8 can desensitize neutrophils to C5a (44). Despite the similarities, there is evidence that the activities of HuMig and IP-10 are not identical. In contrast to what has been reported for rIP-10 (37), we have not thus far found HuMig to act on monocytes. And in assays of neovascularization in mice, rIP-10 but not rHuMig was found to be inhibitory (16).

Given that other CXC and CC chemokines that act on lymphocytes have been found to target also either monocytes or neutrophils, HuMig's T cell specificity is unusual. In this regard, HuMig resembles lymphotactin (3), a recently described cytokine that is similar to the CC chemokines but that lacks two of the four invariant cysteines found in the CC and CXC subfamilies.

While the response to chemokines typically includes a rise in $[Ca^{2+}]_i$ as the result of the activation of a 7–transmembrane-domain G protein–coupled receptor (2), there is a paucity of reports of induction of calcium fluxes in lymphocytes by chemokines. Lymphotactin has been reported to produce a calcium flux in $CD4^+$-depleted thymocytes (3). And LCF, a nonchemokine factor that is chemotactic for $CD4^+$ T cells, monocytes, and eosinophils, has been shown to produce a rise in intracellular calcium in a $CD4^+$ murine T cell hybridoma (45). As far as we are aware, our experiments with rHuMig are the first to show chemokine-induced calcium flux in TIL or in cultured PBL.

A large body of work has established a central role for calcium in signal transduction after stimulation through the

T cell receptor, related both to activation of mature cells (46, 47) and to apoptosis of immature cells (48, 49). A significant difference between HuMig-induced and CD3-induced calcium flux is that the former is transient while the latter is sustained (46, 50). While the former is presumably mediated through trimeric G-protein(s), the latter is the result of activation of receptor- and accessory-molecule–associated tyrosine kinases (51). There is nonetheless evidence that chemokine-dependent and CD3-dependent pathways can interact, since MIP-1α can inhibit the T cell proliferation that follows cross-linking of CD3 (52).

Our calcium flux experiments have demonstrated the importance of COOH-terminal residues for the activity of rHuMig. While, like Mig, the other CXC chemokines generally show a clustering of basic amino acids at their COOH termini, the murine and human Mig proteins are unusual in the lengths of their highly basic COOH termini. The murine and human Migs are the longest of the CXC chemokines, and aligning the Mig sequences with those of the other CXC chemokines reveals that the additional lengths can be attributed to Mig's carboxy terminus (17, 18). The methods of Chou-Fasman (53) and Robson-Garnier (54) as applied by the MacVector software (Eastman Kodak, Rochester, NY) predict that the HuMig COOH-terminal region forms an α-helix (data not shown) consistent with the structural information available for other chemokines (55).

While NH_2-terminal proteolytic processing is well recognized among the chemokines as a modification of functional importance (56), there are few reports of COOH-terminal cleavage. For MGSA/gro, two COOH-terminal residues are removed to produce the mature protein (57) and a NAP-2 variant has been identified lacking several COOH-terminal residues (58), but the extensive COOH-terminal processing shown for HuMig has not been described for other chemokines. We have shown that the CHO/H9 cell line and, after stimulation with IFN-γ, the THP-1 human monocytic line as well as human peripheral blood monocytes produce the same processed forms of HuMig. For the CHO-derived rHuMig, we have established that processing is due to proteolysis that occurs before secretion of rHuMig into the medium. Based on our experiments using protease inhibitors, serine proteases are likely responsible for HuMig's COOH-terminal processing.

Proteolytic processing at COOH-terminal domain basic residues is not unique to HuMig and other chemokines, but has been described for other secreted proteins, such as IFN-γ (59) and tissue factor pathway inhibitor (60). In the case of IFN-γ, as for HuMig, the proteolysis was demonstrated to occur in CHO cells before secretion (59). Little is known about the molecular details of the pathways for this sort of processing. The patterns of HuMig cleavage and our protease inhibitor studies suggest that HuMig is not processed by the recently described KEX2-related proteases that cleave hormones and growth factors at internal dibasic sites (61).

Studies of the CXC chemokines platelet factor 4 and IL-8 have shown that their COOH-terminal domains are of functional importance. COOH-terminal peptides of platelet factor 4 have been shown to possess the immunoregulatory activity (62) and the angiostatic activity (15) that have been ascribed to the full-length protein. For IL-8, deleting the COOH-terminal α helical region led to significant decreases in chemotactic function and in receptor binding (5), although the truncation did not eliminate either activity completely. In contrast, the murine MCP-1 contains a nonbasic COOH-terminal domain of no demonstrated functional importance (63). The mouse MCP-1 differs from its human homologue in having a 49–amino acid serine- and threonine-rich COOH-terminal extension that is heavily glycosylated (63). Removal of this COOH-terminal domain has no effect on the chemotactic activity of the murine MCP-1 as assayed in vitro (63).

Recent work, particularly with IL-8 (64) and MIP1-β (9), has suggested that chemokine binding to both soluble and cell-surface/extracellular matrix–associated glycosaminoglycans is important for chemokine function. Matrix-bound chemokine could provide a fixed gradient up which a cell could move. Both for IL-8 (64) and for platelet factor 4 (65), the COOH-terminal domains have been shown to be essential for this binding to glycosaminoglycans. In addition, it has been proposed, based in part on data for C5a and its receptor, that the basic α-helical domains of the chemokines participate in the initial binding interactions with acidic residues in the extracellular domains of the chemokine receptors (2).

In regard to a nonchemokine cytokine, it has been shown recently that acidic fibroblast growth factor requires binding to heparin or cell-surface heparan sulfate to signal through the fibroblast growth factor receptor (66). We have shown that rHuMig with a large COOH-terminal deletion is not only much diminished in its activity in the calcium flux assay, but also that the truncated rHuMig is unable to block the activity of the full-length protein. This suggests that decreased receptor binding may be the basis for diminished activity shown by the truncated rHuMig. Interactions with cell-surface glycosaminoglycans such as heparan sulfate might be important in the binding of HuMig to its receptor, and these interactions would be expected to be affected by deletion of HuMig's COOH terminus.

Since COOH-terminal cleavage affects the activity of rHuMig, at least with respect to calcium flux in T cells, such processing could well have a regulatory role in vivo. While we have demonstrated that this processing is occurring before secretion for the CHO cells in culture, this does not eliminate the possibility that the susceptibility of HuMig to an inactivating proteolytic cleavage is used in vivo to limit the duration of HuMig's activity after its secretion. In the case of IL-8, for example, it has been reported that inactivation can occur as the result of protease(s) present in serosal fluid (67).

If, in vivo, proteolytic processing of HuMig occurs only before secretion, it raises the question as to what advantage would be conferred by secreting forms of HuMig with

varying specific activities. Considering the likelihood that the truncated forms of HuMig will bind less readily to glycosaminoglycans in extracellular matrix and on cell surfaces, as compared to the full-length HuMig, it is possible that in tissue, as the distance from the HuMig-producing cell increases, the immobilized forms of HuMig would be those more truncated and less active. This would add another dimension to a chemotactic gradient that would now be formed not only by changes in ligand concentration, or density, but also by changes in the specific activities of the immobilized ligands, with specific activities increasing as the distance to the HuMig-producing cell diminishes.

HuMig is induced in macrophages (18) by the lymphocyte product IFN-γ, and HuMig in turn targets activated T cells. Experiments in vivo have demonstrated lymphocyte recruitment into skin at sites of IFN-γ injection (68), and our results make Mig a reasonable candidate for mediating these effects. Similarly, our demonstration that rHuMig can function as a chemotactic factor for TIL makes HuMig a candidate for mediating the lymphocyte chemotaxis induced by supernatants from explanted tumors (69) and for mediating lymphocyte infiltration of tumors in vivo.

Chemokines have been suggested to play key roles in regulating the adhesion and the migration of leukocytes as part of the multistep process of leukocyte trafficking. In particular, chemokines are well-suited to provide an important part of the specificity that is required for the differing patterns of recruitment and recirculation seen for subpopulations of lymphocytes (10). We will be interested in determining what role Mig may have in the trafficking of T lymphocyte subsets and what effects Mig may have on aspects of T cell physiology generally.

We are indebted to F. William Studier for supplying the pET vectors and bacterial strains; to Se-Jin Lee for the pMSXND vector, the parent CHO cells, and helpful discussions; to William Lane and the Harvard Microbiochemistry Facility for NH_2-terminal sequencing and mass spectrometry; to Robert Siliciano for F14.38 and other T cell clones and for the B lymphoblastoid cell lines; to Ashok Srinivisan and James Pipas for the KT3 antibody; to Indu Ambudkar for help with calcium measurements; to Philip Murphy for helpful discussions and critical review of the manuscript; to Daniel Nathans, Chaim Kahana, and Stephen Straus for support and helpful discussions; to Keith Peden, to Thomas Moench, and to the faculty of the 1992 Cold Spring Harbor Laboratory course on protein purification and characterization, for helpful discussions; and to Christine Moss and Corita Wright-Bacon for typing.

The work was begun when Joshua Farber was in the Department of Medicine, Johns Hopkins University School of Medicine, and during a sabbatical in the Department of Molecular Genetics and Virology at the Weizmann Institute of Science.

This work was supported in part by grants CA-48059 and CA-52001 from the National Cancer Institute.

Address correspondence to J. Farber, Laboratory of Clinical Investigation, National Institute of Allergy and Infectious Diseases, Building 10, Room 11N-228, 9000 Rockville Pike, Bethesda, MD 20892. Dr. Vanguri's current address is Department of Neurology, University of Maryland School of Medicine, 6-34F MSTF, 10 S. Pine Street, Baltimore, MD 21201.

Received for publication 14 February 1995 and in revised form 4 May 1995.

References

1. Miller, M.D., and M.S. Krangel. 1992. Biology and biochemistry of the chemokines: a family of chemotactic and inflammatory cytokines. *Crit. Rev. Immunol.* 12:17–46.
2. Murphy, P. 1994. The molecular biology of leukocyte chemoattractant receptors. *Annu. Rev. Immunol.* 12:593–633.
3. Kelner, G.S., J. Kennedy, K.B. Bacon, S. Kleyensteuber, D.A. Largaespada, N.A. Jekins, N.G. Copeland, J.F. Bazan, K.W. Moore, T.J. Schall, and A. Zlotnik. 1994. Lymphotactin: a cytokine that represents a new class of chemokine. *Science (Wash. DC).* 266:1395–1399.
4. Hebert, C.A., R.V. Vitangcol, and J.B. Baker. 1991. Scanning mutagenesis of interleukin-8 identifies a cluster of residues required for receptor binding. *J. Biol. Chem.* 266: 18989–18994.
5. Clark-Lewis, I., C. Schumacher, M. Baggiolini, and B. Moser. 1991. Structure-activity relationships of interleukin-8 determined using chemically synthesized analogs. Critical role of NH_2-terminal residues and evidence for uncoupling of neutrophil chemotaxis, exocytosis, and receptor binding activities. *J. Biol. Chem.* 266:23128–23134.
6. Schall, T.J., K. Bacon, K.J. Toy, and D.V. Goeddel. 1990. Selective attraction of monocytes and T lymphocytes of the memory phenotype by cytokine RANTES. *Nature (Lond.).* 347:669–672.
7. Taub, D.D., K. Conlon, A.R. Lloyd, and J.J. Oppenheim. 1993. Preferential migration of activated $CD4^+$ and $CD8^+$ T cells in response to Mip-1α and Mip-1β. *Science (Wash. DC).* 260:355–358.
8. Schall, T.J., K. Bacon, R.D.R. Camp, J.W. Kaspari, and D.V. Goeddel. 1993. Human macrophage inflammatory protein α (Mip-1α) and Mip-1β attract distinct populations of lymphocytes. *J. Exp. Med.* 177:1821–1825.

9. Tanaka, Y., D.H. Adams, and S. Shaw. 1993. Proteoglycans on endothelial cells present adhesion-inducing cytokines to leukocytes. *Immunol. Today.* 13:291–295.
10. Springer, T.A. 1994. Traffic signals for lymphocyte recirculation and leukocyte emigration: the multistep paradigm. *Cell.* 76:301–314.
11. Graham, G.J., E.G. Wright, R. Hewick, S.D. Wolpe, N.M. Wilkie, D. Donaldson, S. Lorimore, and I.B. Pragnell. 1990. Identification and characterization of an inhibitor of haemopoietic stem cell proliferation. *Nature (Lond.).* 344:442–444.
12. Broxmeyer, H.E., B. Sherry, S. Cooper, L. Lu, R. Maze, M.P. Beckmann, A. Cerami, and P. Ralph. 1993. Comparative analysis of the human macrophage inflammatory protein family of cytokines (chemokines) on proliferation of human myeloid progenitor cells. *J. Immunol.* 150:3448–3458.
13. Baggiolini, M., and C.A. Dahinden. 1994. CC chemokines in allergic inflammation. *Immunol. Today.* 15:127–133.
14. Koch, A.E., P.J. Polverini, S.L. Kunkel, L.A. Harlow, L.A. Pietra, V.M. Elner, S.G. Elner, and R.M. Strieter. 1992. Interleukin-8 as a macrophage-derived mediator of angiogenesis. *Science (Wash. DC).* 258:1798–1801.
15. Maione, T.E., G.S. Gray, J. Petro, A.J. Hunt, A.C. Donner, S.I. Bauer, H.F. Carson, and R.J. Sharpe. 1990. Inhibition of angiogenesis by recombinant human platelet factor-4 and related peptides. *Science (Wash. DC).* 247:77–79.
16. Angiolillo, A.L., C. Sgadari, D.D. Taub, F. Liao, J.M. Farber, S. Maheshwari, H.K. Kleinman, G.H. Reaman, and G. Tosato. 1995. Human interferon-inducible protein 10 is a potent inhibitor of angiogenesis in vivo. *J. Exp. Med.* 182:155–162.
17. Farber, J.M. 1990. A macrophage mRNA selectively induced by γ-interferon encodes a member of the platelet factor 4 family of cytokines. *Proc. Natl. Acad. Sci. USA.* 87:5238–5242.
18. Farber, J.M. 1993. HuMIG: a new human member of the chemokine family of cytokines. *Biochem. Biophys. Res. Commun.* 192:223–230.
19. Tashiro, K., H. Tada, R. Heilker, M. Shirozu, T. Nakano, and T. Honjo. 1993. Signal sequence trap: a cloning strategy for secreted proteins and type I membrane proteins. *Science (Wash. DC).* 261:600–603.
20. Studier, F.W., A.H. Rosenberg, J.J. Dunn, and J.W. Dubendorff. 1990. Use of T7 RNA polymerase to direct expression of cloned genes. *Methods Enzymol.* 185:60–89.
21. Lee, S.J., and D. Nathans. 1988. Proliferin secreted by cultured cells binds to mannose 6-phosphate receptors. *J. Biol. Chem.* 263:3521–3527.
22. Laemmli, U.K. 1970. Cleavage of structural proteins during the assembly of the head of the bacteriophage T4. *Nature (Lond.).* 227:680–685.
23. Schagger, H., and G. Von Jagow. 1987. Tricine-sodium dodecyl sulfate-polyacrylamide gel electrophoresis for the separation of proteins in the range from 1 to 100 kDa. *Anal. Biochem.* 166:368–397.
24. Blum, H., H. Beier, and H.J. Gross. 1987. Improved silver staining of plant proteins, RNA and DNA in polyacrylamide gels. *Electrophoresis.* 8:93–99.
25. Smith, P.K., R.I. Krohn, G.T. Hermanson, A.K. Mallia, F.H. Gartner, M.D. Provenzano, E.K. Fujimoto, N.M. Goeke, B.J. Olson, and D.C. Klenk. 1985. Measurement of protein using bicinchoninic acid. *Anal. Biochem.* 150:76–85.
26. Yannelli, J.R. 1991. The preparation of effector cells for use in the adoptive cellular immunotherapy of human cancer. *J. Immunol. Methods.* 139:1–16.
27. Kruisbeek, A.M., and E.M. Shevach. 1991. Proliferative assays for T cells. *In* Current Protocols in Immunology. J.E. Coligan, A.M. Krusibeek, D.H. Margulies, E.M. Shevach, and W. Strober, editors. John Wiley & Sons, New York. 3.12.1–3.12.14.
28. Grynkiewcz, G., M. Poenie, and R.Y. Tsien. 1985. A new generation of Ca^{2+} indicators with greatly improved fluorescence properties. *J. Biol. Chem.* 260:3440–3450.
29. Clark, R.A., and W.M. Nauseef. 1991. Isolation and functional analysis of neutrophils. *In* Current Protocols in Immunology. J.E. Coligan, A.M. Krusibeek, D.H. Margulies, E.M. Shevach, and W. Strober, editors. John Wiley & Sons, New York. 7.23.1–7.23.3.
30. Falk, W.R., R.H.J. Goodwin, and E.J. Leonard. 1980. A 48-well microchemotaxis assembly for rapid and accurate measurement of leukocyte migration. *J. Immunol. Methods.* 33: 239–247.
31. MacArthur, H., and G. Walter. 1984. Monoclonal antibodies specific for the carboxy terminus of simian virus 40 large T antigen. *J. Virol.* 52:483–491.
32. Bjorn, G., and P.O. Seglen. 1980. Differential effects of proteinase inhibitors and amines on the lysosomal and non-lysosomal pathways of protein degradation in isolated rat hepatocytes. *Biochim. Biophys. Acta.* 632:73–86.
33. Denison, M.R., P.W. Zoltick, S.A. Hughes, B. Giangreco, A.L. Olson, S. Perlman, J.L. Leibowitz, and S.R. Weiss. 1992. Intracellular processing of the N-terminal ORF la proteins of the coronavirus MHV-A59 requires multiple proteolytic events. *Virology.* 189:274–284.
34. Zhirov, O., and A.G. Bukrinskaya. 1984. Nucleoproteins of animal influenza viruses in contrast to those of human strains, are not cleaved in infected cells. *J. Gen. Virol.* 65:1127–1134.
35. Richmond, A., E. Balentien, H.G. Thomas, G. Flaggs, D.E. Barton, J. Spiess, R. Bordoni, U. Francke, and R. Derynk. 1988. Molecular characterization and chromosomal mapping of melanoma growth stimulatory activity, a growth factor structually related to β-thromboglobulin. *EMBO (Eur. Mol. Biol. Organ.) J.* 7:2025–2033.
36. Stanhope, P.E., A.Y. Liu, W. Pavlat, P.M. Pitha, M.L. Clements, and R.F. Siliciano. 1993. An HIV-1 envelope protein vaccine elicits a functionally complex human $CD4^+$ T cell response that includes cytolytic T lymphocytes. *J. Immunol.* 150:4672–4686.
37. Taub, D.D., A.R. Lloyd, K. Conlon, J.M. Wang, J.R. Ortaldo, A. Harada, K. Matsushima, D.J. Kelvin, and J.J. Oppenheim. 1993. Recombinant human interferon-inducible protein 10 is a chemoattractant for human monocytes and T lymphocytes and promotes T cell adhesion to endothelial cells. *J. Exp. Med.* 177:1809–1814.
38. Zachariae, C.O. 1993. Chemotactic cytokines and inflammation. Biological properties of the lymphocyte and monocyte chemotactic factors ELCF, MCAF and IL-8. *Acta Dermatoveneriol. (Suppl).* 181:1–37.
39. Carr, M.W., S.J. Roth, E. Luther, S.S. Rose, and T.A. Springer. 1994. Monocyte chemoattractant protein 1 acts as a T-lymphocyte chemoattractant. *Proc. Natl. Acad. Sci. USA.* 91:3652–3656.
40. Wilkinson, P.C., and I. Newman. 1992. Identification of IL-8 as a locomotor attractant for activated human lymphocytes in mononuclear cell cultures with anti-CD3 or purified protein derivative of *Mycobacterium tuberculosis. J. Immunol.* 149:2689–

2694.
41. Luster, A.D., J.C. Unkeless, and J.V. Ravetch. 1985. γInterferon transcriptionally regulates an early-response gene containing homology to platelet proteins. *Nature (Lond.)*. 315: 672–676.
42. Vanguri, P., and J.M. Farber. 1990. Identification of CRG-2: an interferon-inducible mRNA predicted to encode a murine monokine. *J. Biol. Chem.* 265:15049–15057.
43. Didsburg, J.R., R.J. Uhing, E. Tornhave, C. Geraard, N. Gerard, and R. Snyderman. 1991. Receptor class desensitization of leukocyte chemoattractant receptors. *Proc. Natl. Acad. Sci. USA*. 88:11564–11568.
44. Gao, J.-L., E.L. Becker, R.J. Freer, N. Muthukumaraswamy, and P.M. Murphy. 1994. A high potency nonformylated peptide agonist for the phagocyte *N*-formylpeptide chemotactic receptor. *J. Exp. Med.* 180:2191–2197.
45. Cruikshank, W.W., D.M. Center, N. Nisar, M. Wu, B. Natke, A.C. Theodore, and H. Kornfeld. 1994. Molecular and functional analysis of a lymphocyte chemoattractant factor: association of biologic function with CD4 expression. *Proc. Natl. Acad. Sci. USA*. 91:5109–5113.
46. Imboden, J.B., A. Weiss, and J. Stobo. 1985. The antigen receptor on a human T cell line initiates activation by increasing cytoplasmic free calcium. *J. Immunol.* 134:663–665.
47. Nisbet-Brown, E., R.K. Cheung, J.W.W. Lee, and E.W. Gelfund. 1985. Antigen dependent increase in cytosolic free calcium in specific human T-lymphocyte clones. *Nature (Lond.)*. 316:545–547.
48. Smith, C.A., G.T. Williams, R. Kingston, E.J. Jenkinson, and J.J.T. Owen. 1989. Antibodies to CD3/T-cell receptor complex induce death by apoptosis in immature T cells in thymic cultures. *Nature (Lond.)*. 337:181–184.
49. McConkey, D.J., P. Hartzell, P. Nicotera, and S. Orrenius. 1989. Calcium-activated DNA fragmentation kills immature thymocytes. *FASEB J.* 3:1843–1849.
50. McConkey, D.J., P. Hartzell, J.F. Amador-Perez, S. Orrenius, and M. Jondal. 1989. Calcium-dependent killing of immature thymocytes by stimulation via the CD3/T cell receptor complex. *J. Immunol.* 143:1801–1806.
51. Weiss, A., and D.R. Littman. 1994. Signal transduction by lymphocyte antigen receptors. *Cell*. 76:263–274.
52. Zhou, Z., Y.-J. Kim, K. Pollok, J. Hurtado, J.-K. Lee, H.E. Broxmeyer, and B.S. Kwon. 1993. Macrophage inflammatory protein-1α rapidly modulates its receptors and inhibits the anti-CD3 mAb-mediated proliferation of T lymphocytes. *J. Immunol.* 151:4333–4341.
53. Chou, P.Y., and G.D. Fasman. 1978. Empirical predictions of protein conformations. *Annu. Rev. Biochem.* 47:251–276.
54. Garnier, J., D.J. Osguthorpe, and B. Robson. 1978. Analysis of the accuracy and implications of simple methods for predicting the secondary structure of globular proteins. *J. Mol. Biol.* 120:97–120.
55. Clore, G.M., E. Apella, M. Yamada, K. Matsushima, and A.M. Gronenhorn. 1989. Determination of the secondary structure of interleukin-8 by nuclear magnetic resonance spectroscopy. *J. Biol. Chem.* 264:18907–18911.
56. Van dame, J., J. Van Beeumen, R. Conings, B. Decock, and A. Billiau. 1989. Purification of granulocyte chemotactic peptide/interleukin-8 reveals N-terminal sequence heterogeneity similar to that of β-thromboglobulin. *Eur. J. Biochem.* 181:337–344.
57. Derynk, R., E. Balentien, J.H. Han, H.G. Thomas, D. Wen, A.K. Samantha, C.O. Zachariae, P.R. Griffin, R. Brachmann, W.L. Wong, et al. 1990. Recombinant expression, biochemical characterization, and biological activities of the human MGSA/gro protein. *Biochemistry*. 29:10225–10233.
58. Brandt, E., F. Petersen, and H.D. Flad. 1993. A novel molecular variant of the neutrophil-activating peptide NAP-2 with enhanced biological activity is truncated at the C-terminus: identification by antibodies with defined epitope specificity. *Mol. Immunol.* 30:979–991.
59. Curling, E.M.A., P.M. Hayter, A.J. Baines, A.T. Bull, K. Gull, P.G. Strange, and N. Jenkins. 1990. Recombinant human interferon-γ. Differences in glycosylation and proteolytic processing lead to heterogeneity in batch culture. *Biochem. J.* 272:333–337.
60. Wan, T.-C., K.K. Kretzmer, M. Palmier, K.C. Day, M.D. Huang, D.J. Welsch, C. Lewis, R.A. Wolfe, J.F. Zobel, G.W. Lange, et al. 1992. Comparison of recombinant tissue factor pathway inhibitors expressed in human SK hepatoma, mouse C127, baby hamster kidney, and chinese hamster ovary cells. *Thromb. Hemostasis*. 68:54–59.
61. Barr, P.J. 1991. Mammalian subtilisins: the long-sought dibasic processing endoproteases. *Cell*. 66:1–3.
62. Zucker, M.B., I.R. Katz, G.J. Thorbecke, D.C. Milot, and J. Holt. 1989. Immunoregulatory activity of peptides related to platelet factor 4. *Proc. Natl. Acad. Sci. USA*. 86:7571–7574.
63. Ernst, C.A., Y.J. Zhang, P.R. Hancock, B.J. Rutledge, C.C. Corless, and B.J. Rollins. 1984. Biochemical and biologic characterization of murine monocyte chemoattractant protein-1. *J. Immunol.* 152:3541–3549.
64. Webb, L.M.C., M.U. Ehrengruber, I. Clark-Lewis, M. Baggiolini, and A. Rot. 1993. Binding to heparan sulfate or heparin enhances neutrophil responses to interleukin 8. *Proc. Natl. Acad. Sci. USA*. 90:7158–7162.
65. Loscallzo, J., B. Melnick, and R.I. Handin. 1985. The interaction of platelet factor four and glycosaminoglycans. *Arch. Biochem. Biophys.* 240:446–455.
66. Spivak-Kroizman, T., M.A. Lemmon, I. Dikic, J.E. Ladbury, D. Pinchasi, J. Huang, M. Jaye, G. Crumley, J. Schlessinger, and I. Lax. 1994. Heparin-induced oligomerization of FGF molecules is responsible for FGF receptor dimerization, activation, and cell proliferation. *Cell*. 79:1015–1024.
67. Ayesh, S.K., Y. Azar, B.M. Babior, and Y. Matzner. 1993. Inactivation of interleukin-8 by the C5a-inactivating protease from serosal fluid. *Blood*. 81:1424–1427.
68. Issekutz, T.B., J.M. Stoltz, and P.V.D. Meide. 1988. Lymphocyte recruitment in delayed-type hypersensitivity. The role of IFN-γ. *J. Immunol.* 140:2989–2993.
69. Averbook, B.J., J.P. Wei, D.M. Perry-Lalley, S.A. Rosenberg, and J.C. Yang. 1993. A tumor-elaborated supernatant factor chemotactic for IL-2 expanded tumor infiltrating T-lymphocytes. *Lymphokine Cytokine Res.* 12:1–8.